Optical characterization of vacuum evaporated cadmium sulfide films

U. Pal [a,*], R. Silva-González [a], G. Martínez-Montes [a], M. Gracia-Jiménez [a], M.A. Vidal [b], Sh. Torres [b]

[a] *Instituto de Física, Universidad Autónoma de Puebla, Apdo. Postal J-48, Puebla, Puebla 72570, México*
[b] *Instituto de Investigación en Comunicación Optica, Universidad Autónoma de San Luis Potosí, Alvaro Obregón #64, San Luis Potosí, 78000, México*

Abstract

The optical constants (n,k) of cadmium sulfide (CdS) thin films were determined in the spectral range of 0.55 μm to 1.80 μm from the optical absorption and transmittance measurements. The optical band gap (E_g) was determined for the films deposited at different substrate temperatures. Scanning electron microscopy (SEM), energy dispersive X-ray (EDX) analysis and X-ray diffraction (XRD) techniques were used to determine the morphology, composition, crystalline structure and crystallite size of the films. Evaporated CdS films show a predominant hexagonal phase with small crystallites. The optical band gap values of the films varied from 2.38 to 2.41 eV depending on the substrate temperature. It has been observed that the band gap and refractive index of the films have a close relationship with the size of the crystallites. The lower estimated value of band gap of the films is explained considering the effects of excitons and (or) some impurities. © 1997 Elsevier Science S.A.

Keywords: Cadmium sulphide; Evaporation; Optical properties

1. Introduction

Thin films of cadmium sulfide (CdS) are of considerable interest for their efficient use in the fabrication of solar cells [1,2] and other optoelectronic devices [3]. There exists a vast literature [4–8] comprising experimental and theoretical investigations of electronic band structure and related properties of this compound. The study of optical constants of CdS near the fundamental absorption edge is interesting in view of the importance of this material as a "model" photoconductor. Moreover, the study of optical constants in the sub band gap region is often of interest for using this material in solar cells and in other optoelectronic device designs. Accurate knowledge of the refractive index and absorption coefficient of semiconductors is indispensable for the design and analysis of various optoelectronic devices. Although there have been many reports on the optical constants of CdS [9–11], the current state of available data in the visible-to-ultraviolet region seems to be less than adequate especially in the context of structural phase transition in thin films.

Several workers have studied the optical properties of CdS films deposited by different techniques like chemical bath deposition (CBD) [12,13], thermal evaporation [14–18], molecular beam epitaxy (MBE), [19,20] etc. Though by epitaxial techniques it is possible to grow CdS films of single phase (either as cubic or hexagonal), there appeared generally a mixed phase for the films deposited either by CBD or by thermal evaporation. The anomalies on the estimated band gap values for the films deposited either by CBD or thermal evaporation techniques are very often explained by the variation of sulfur content and hence a crystalline phase transformation in the films [21]. However, the picture is not clear until now. For further understanding of this phenomenon, we studied the optical properties of CdS films deposited at different substrate temperatures. X-ray diffraction (XRD) studies have been performed to monitor the changes of the crystalline structure with deposition temperature. Variations of band gap and refractive index of the films are seen to be less sensitive to the composition. The effects of crystallite size and crystalline phase composition on the optical constants are presented.

2. Experimental

Thin films of CdS were deposited on thoroughly cleaned glass substrates at different substrate temperatures (T_s)
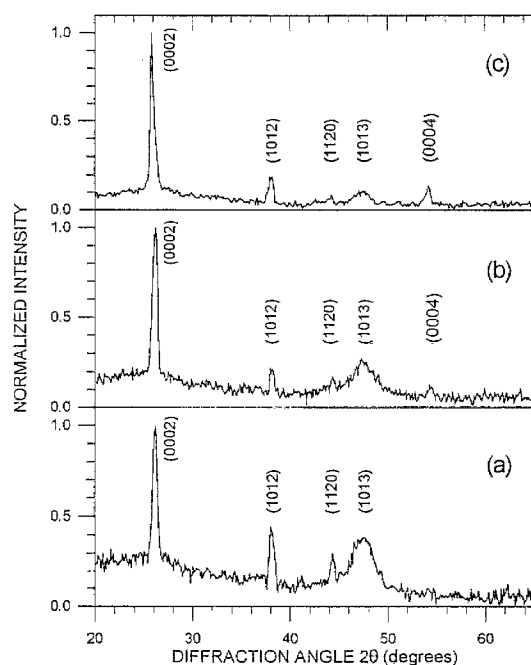
---

* Corresponding author.

Fig. 1. XRD spectra of CdS films deposited at a) $T_s = 393$ K, b) $T_s = 473$ K and c) $T_s = 623$ K.

using a JEOL, JEE-400 evaporation system. The CdS powder (Balzers, 99.999%) was evaporated from a tungsten boat inside the deposition chamber and maintained at a pressure of about 10^{-4} Pa. The deposition rate was maintained at 120 nm min^{-1}. After removal from the deposition chamber, the films were exposed to air for a few days prior to the characterizations. The composition and morphology of the films were studied by a JEOL, JSM 5400LV scanning electron microscope with NORAN system. It was observed that the composition of the films varies with the substrate temperature. XRD patterns of the films were recorded by a Phillips (PW 3710) X-ray diffractometer. There always appeared an intense XRD peak with a broader background which was assigned to the (0002) reflection of the hexagonal phase. With the increase of substrate temperature, a complex evolution of other peaks also appeared. However, with the increase of substrate temperature, an increase of hexagonal phase is evident from the appearance of other well defined hexagonal re-

flections. In Fig. 1, the XRD patterns of CdS films deposited at 393 K, 473 K and 623 K are presented. The calculated interplanar spacings and the corresponding probable indices are presented in Table 1. The average size of the crystallites was determined from the (0002) peak using the Scherrer formula:

$$P = (K\lambda)/\beta \cos \theta \qquad (1)$$

after correction for the instrumental spectral broadening [22]. Where P is the crystallite size, λ is the wavelength of the X-rays ($\lambda = 1.54056$ in the present study), θ is the Bragg angle, β the width of the peak at the half of the maximum peak intensity and K is a constant of proportionality usually taken as equal to unity.

The absorption and transmission measurements of the films relative to an uncovered glass substrate were done by a Cary-5 double monochromator recording spectrophotometer. The absorption starts with a slow rise in the low-energy region followed by a sharp rise in the higher energy region.

3. Results and discussions

The as deposited films were smooth, reflective, adherent and bright orange in color. It has been observed from the XRD patterns of the CdS films deposited at different temperatures that all of the films have a hexagonal structure with a preferred orientation of (0002) axis perpendicular to the substrate. Due to the fact that the most intense peaks of the cubic and of the hexagonal phase coincide in the diffraction angle position within 1%, the interpretation of XRD spectra became a difficult task. However, with the increase of substrate temperature, the appearance of hexagonal phase increased in the films. The average crystallite size value in the films increased up to $T_s = 473$ K and then decreased gradually. The scanning electron microscopy (SEM) pictures of the films deposited at $T_s = 300$ K (RT), $T_s = 473$ K and $T_s = 623$ K are shown in Fig. 2. The increase of the crystallite size up to about 473 K substrate temperature is also revealed from the micrographs. However, the crystallite sizes revealed from the SEM pictures are higher than the average crystallite size values calcu-

Table 1

Interplanar spacing and their corresponding probable indices for the XRD peaks of the CdS films deposited at different substrate temperatures

| $T_s = 300$ K (RT)		$T_s = 393$ K		$T_s = 473$ K		$T_s = 523$ K		$T_s = 573$ K		$T_s = 623$ K	
d (nm)	hkl	d (nm)	hkl	d (nm)	hkl	d (nm)	hkl	d (nm)	hkl	d (nm)	hkl
0.376	1010	–	–	–	–	–	–	–	–	–	–
0.3401	0002	0.3418	0002	0.3414	0002	0.3412	0002	0.3400	0002	0.3409	0002
0.2362	1012	0.2363	1012	0.2363	1012	0.2359	1012	0.2358	1012	0.2370	1012
–	–	0.2046	1120	0.2043	1120	0.2048	1120	0.2039	1120	0.2050	1120
–	–	0.1911	1013	0.1923	1013	0.1918	1013	0.1916	1013	0.1921	1013
–	–	–	–	–	–	0.1729	2021	–	–	–	–
0.1689	0004	–	–	0.1692	0004	0.1690	0004	0.1688	0004	0.1690	0004
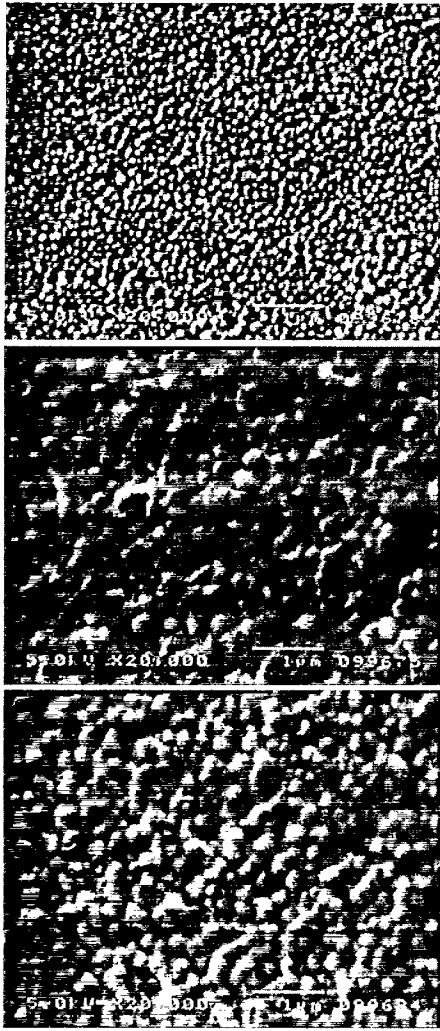
Fig. 2. SEM photographs of CdS films deposited at a) T_s = 300 K (RT), b) T_s = 473 K and c) T_s = 623 K.

lated from the XRD peaks. Such a difference might be due to the presence of some amorphous phase in the films along with their predominant crystalline phase.

The introduction of stacking faults in evaporated hexagonal films leads to the formation of the cubic phase [23]. Because CdS possesses a low stacking-fault energy, fault formation can take place during the deposition itself or after deposition via plastic deformation resulting from the difference in thermal expansion coefficient between the film and the substrate. The appearance of cracks in some of the films deposited at room temperature (RT) may also be attributed to a high tensile stress in the films. A similar observation has also been reported by other workers [12] for their CBD films.

The energy dispersive X-ray (EDX) analysis results show that the films are more or less stoichiometric. The ratio of Cd to S (atom percent) approaches to 1.0 as the substrate temperature approaches to 500 K. However, all the films had some Cd excess over S. As we could not detect any oxygen-related emission in the Auger electron

spectra of the films, such excess Cd might have incorporated as some metallic inclusions in the films.

The plots of transmission T against wavelength λ are found to show the usual interference pattern of a high index film in the range of low absorption, which may be described in the case of semi-infinite substrate, by the relations given by Manifacier et al. [24].

The maxima and minima in the T–λ plot occur when:

$$4.n.t/\lambda = M \tag{2}$$

where M represents the order number and t is the thickness of the film. The thicknesses of the films were determined from the interference maxima and minima of the transmission spectra. The refractive index n may be computed from the relation [24–26]:

$$n^2 = \left(n_a^2 + n_g^2\right)/2 + 2n_a n_g T''$$
$$+ \left\{\left(n_a^2 + n_g^2 + 4n_a n_g T''\right)^2/4 - n_a^2 n_g^2\right\}^{1/2} \tag{3}$$

where $T'' = (T_{max} - T_{min})/(T_{max}T_{min})$ and n_a, n_g are the refractive indices of air and substrate respectively. T_{max} and T_{min} represent the envelopes of the maxima and minima positions of the T–λ curve. An exponential variation in T with the absorption coefficient α $(= 4\pi k/\lambda)$ is most probable near the absorption edge. In the strong absorption region, α may be determined from:

$$T = A\exp(-\alpha t) \tag{4}$$

where

$$A = \left\{16 n_a n_g (n^2 + k^2)\right\}$$
$$/\left\{(n_a + n)^2 + k^2\right\}\left\{(n_g + n)^2 + k^2\right\} \tag{5}$$

and k is the extinction coefficient. A is found to be nearly equal to 0.7 at the absorption edge.

The relation between α and incident photon energy $h\nu$ can be written as [26,27]:

$$\alpha h\nu = C_1\left(h\nu - E_g^d\right)^{1/2} \tag{6}$$

$$\alpha h\nu = C_2\left(h\nu - E_g^i\right)^2 \tag{7}$$

for allowed direct and indirect electron transitions between the valence and conduction band respectively, where C_1 and C_2 are two constants, E_g^d and E_g^i are the direct and indirect band gaps respectively.

Fig. 3 and Fig. 4 show the variation of the refractive index n and absorption constant k respectively with incident wavelength for the films deposited at different substrate temperatures. The results for the different specimen of the same set of films were reproducible to within 1%. It is interesting to note that the refractive index n of the films follows the similar trend of variation with the substrate temperature as that of the band gap. With the increase of crystallite size value, the refractive index value increased. For illustration, the variations of band gap, crystallite size and refractive index at 1000 nm with
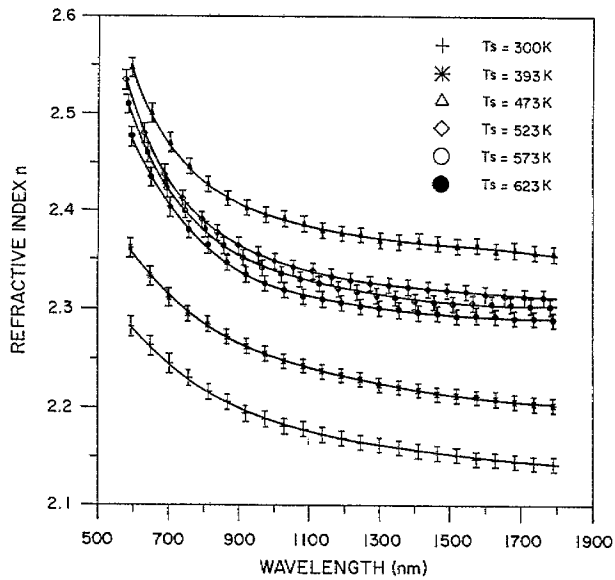
Fig. 3. Variation of refractive index n with wavelength for the CdS films deposited at different substrate temperatures.

Fig. 5. Variation of band gap, average crystallite size and refractive index n (at 1000 nm) with substrate temperature.

substrate temperature are shown in Fig. 5. Both the band gap and refractive index approach closer to their corresponding reported values for the bulk crystals for the films deposited at 473 K. A similar increase of n with T_s has also been observed by Ehsan and Tomlin [27]. Though the refractive index values of our films differ markedly from the reported values for the evaporated CdS films grown on quartz substrates [15], the value for the films deposited at $T_s = 473$ K agree more or less with the single crystal refractive index values of Ninomiya and Adachi [6] and Lisitsa et al. [28].

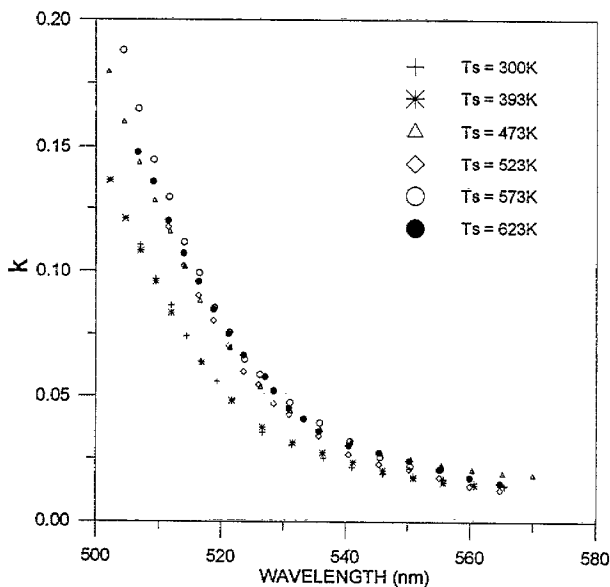The absorption coefficients for the CdS films follow a

good fit with the $(\alpha h\nu)^2$ vs. $h\nu$ plot. The direct band gap values obtained for the films are listed in Table 2. The $(\alpha h\nu)^2$ vs. $h\nu$ plots for the films deposited at different substrate temperatures are shown in Fig. 6. Up to a

Fig. 4. Variation of absorption constant k with wavelength for the CdS films deposited at different substrate temperatures.

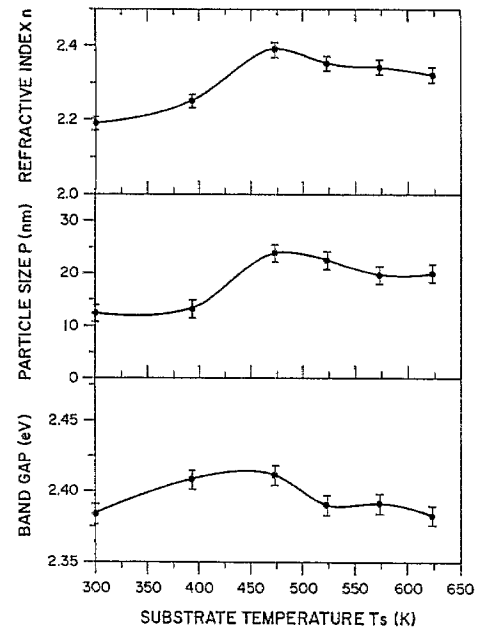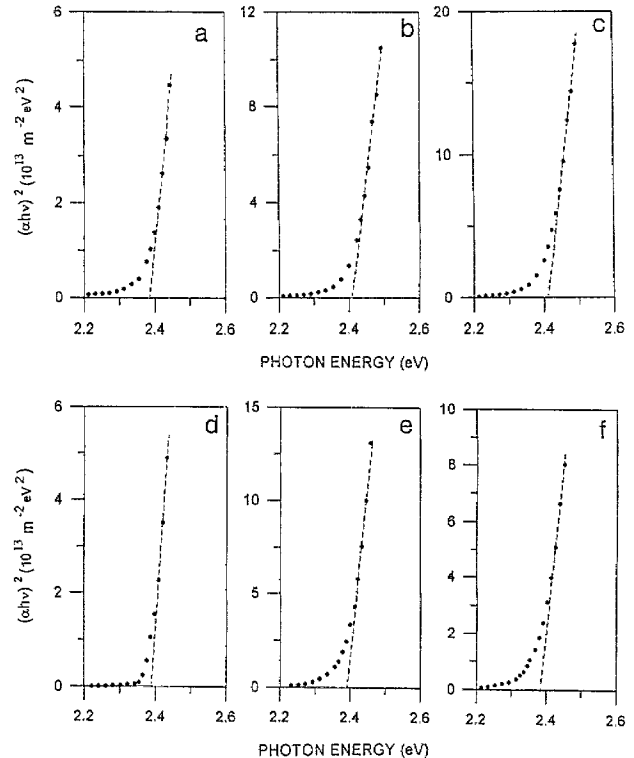Fig. 6. The $(\alpha h\nu)^2$ vs. $h\nu$ plots for the CdS films deposited at a) $T_s = 300$ K (RT), b) $T_s = 393$ K c) $T_s = 473$ K, d) $T_s = 523$ K, e) $T_s = 573$ K, and f) $T_s = 623$ K.

Table 2
Comparison of band gap E_g and refractive index n of the CdS films deposited at different substrate temperatures with their composition and crystallite size. The subscripts and superscripts associated to the bulk parameters represent the phase and references from where they were taken respectively

Substrate temperature T_s (K)	Film thickness t (nm)	Cd/S (atom %)	Crystallite size P (nm)	E_g (eV)	Refractive index n (at 1000 nm)
300	1760 ± 10	1.06	12.4	2.38	2.19
393	1003 ± 15	1.05	13.1	2.41	2.25
473	995 ± 20	1.02	23.8	2.41	2.39
523	1840 ± 15	1.02	22.4	2.39	2.35
573	1137 ± 35	1.03	19.6	2.39	2.34
623	1302 ± 15	1.04	19.9	2.38	2.32
Bulk	–	–	–	2.48_H^6	2.36_H^6
	–	–	–	2.38_H^8	2.35_C^{15}

substrate temperature of about 473 K, the band gap value increased, while for higher substrate temperatures, it gradually decreased. A similar increase of band gap of up to 473 K has also been observed by Ashour et al. [17] for their evaporated CdS films. However, their estimated band gap values were remarkably lower than the other reported values. Our estimated band gap values are lower than the reported value of Birman [29] and Ninomiya and Adachi [6] but close to the values given by Dutton [9] for their CdS crystals. Though, very often, the transition from hexagonal to cubic phase was assigned as the reason for the decrease of band gap, it was concluded [27,30] that the difference between the wurtzite and zinc blende crystal potentials only vary slightly and the band gap energies differ only by a small amount (about 0.1 eV). Lower band gap values of CBD films which have been annealed in a S_2 atmosphere have been reported by several workers [21,31] and have been explained either by considering a phase transition or the disorder and defect contributions.

Though the appearance of the cubic phase along with the hexagonal phase may be a reason for the lower value of the band gap [32], strain, imperfections [30,33] and excitonic effects might have some influence on it. It is well known that the excitonic interaction in the neighborhood of the lowest direct band edge dramatically changes the

Fig. 7. Band edge PL spectrum of CdS film deposited at 473 K.

optical spectra. A complex structure in the strong absorption region is attributed to excitons by several workers [9,30,33]. Observations of Balkansi and Broser [34] and Diemer and Hoogenstraaten [35] of possible exciton diffusion, raise the possibility that exciton transitions comprise part of all the familiar absorption in the neighborhood of 510 nm (2.38 eV). A relationship of this structure to the absorption "tail" defines the fundamental absorption edge in thin films. From the photoluminescence (PL) studies at low temperature, we could detect about four closely spaced peaks near the band edge and the width of the overall peak was about 30 meV. However, at RT, the fine structures were not resolved and the band edge peak broadened more. A near band edge PL spectrum of CdS film deposited at 473 K is shown in Fig. 7 for illustration. The details of PL measurements on different samples are in progress and will be presented later.

4. Conclusions

The CdS thin films deposited by thermal evaporation are shown to have a predominant hexagonal phase and might have some cubic phase mixed with it. With the increase of substrate temperature, the fraction of hexagonal phase in the films increases.

The films deposited by thermal evaporation are more or less stoichiometric. The films deposited at about 473 K substrate temperature have the optimum value of band gap, refractive index and crystallite size.

The lower values of band gap of the films can be explained considering mainly the effect of impurities and excitonic transitions in them. However, there might have been some contribution from the presence of cubic phase in the predominant hexagonal phase. Room temperature PL spectra revealed a broad band edge emission for the films deposited at 473 K. However, for the other films, the band edge emissions were either of very low intensity or missing. This also justifies our argument about the contribution of excitons and impurities on the lower estimated value of the optical band gap.
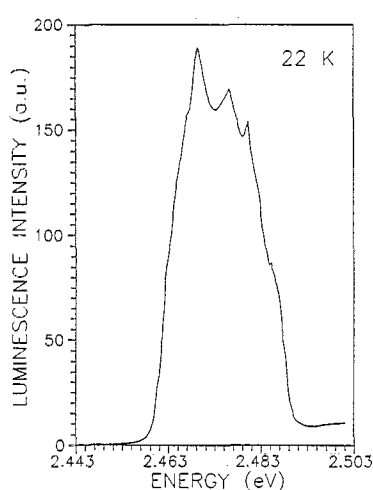
Acknowledgements

References

[1] T.L. Chu, S.S. Chu, J. Britt, C. Ferekids, C. Wang, C.Q. Wu, H.S. Ullal, IEEE Electron Dev. Lett. EDL-13 (1992) 303.

[2] J. Britt, C. Ferekids, Appl. Phys. Lett. 62 (1993) 2851.

[3] I. Broser, Ch. Fricke, B. Lummer, R. Heitz, H. Perls, A. Hoffmann, J. Cryst. Growth 117 (1992) 788.

[4] A. Zunger, A.J. Freeman, Phys. Rev. B17 (1978) 4850.

[5] R.N. Euwema, D.J. Stukel and T.C. Collins, in Computational Methods in Band Theory, P.M. Marcus, J.F. Janak and A.R. Wittium (Eds.), Plenum, New York, 1971.

[6] S. Ninomiya, S. Adachi, J. Appl. Phys. 78 (1995) 1183.

[7] H.R. Philipp, E.A. Taft, Phys. Rev. 113 (1959) 1002.

[8] M. Cardona, D.L. Greenaway, Phys. Rev. 131 (1963) 98.

[9] D. Dutton, Phys. Rev. 112 (1958) 785.

[10] D.G. Thomas, J.J. Hopfield, Phys. Rev. 116 (1959) 573.

[11] M. Cardona, Solid State Commun. 1 (1963) 109.

[12] W.J. Danaher, L.E. Lyons, G.C. Morris, Solar Energy Matter. 12 (1985) 137.

[13] A. Mendoza-Galván, G. Martinez, R. Cozada-Morales, J. Appl. Phys. 80 (1996) 3333.

[14] E. Mollow, Reichsber. Physik 1 (1944) 1.

[15] J.F. Hall Jr., J. Optical Soc. Am. 46 (1956) 1013.

[16] T. Nakanishi, K. Ito, Sol. Energy Mater. Sol. Cells 35 (1994) 171.

[17] A. Ashour, N. El-Kadry, S.A. Mahmoud, Thin Solid Films 269 (1995) 117.

[18] S. Duke, R.W. Miles, P.C. Pande, S. Spoor, B. Ghosh, P.K. Datta, M.J. Carter, R. Hill, J. Cryst. Growth 159 (1996) 916.

[19] Ph. Hofmann, K. Horn, A.M. Bradshaw, R.L. Johnson, D. Fuchs, M. Cardona, Phys. Rev. B47 (1993) 1639.

[20] W.G. Wilke, R. Seedorf, K. Horn, J. Vac. Sci. Technol. B7 (1989) 807.

[21] L. Hernandez, O. de Melo, O. Zelaya-Angel, R. Lozada-Morales, J. Electrochem. Soc. 141 (1994) 3238.

[22] U. Pal, S. Saha, B.K. Samantaray, H.D. Banerjee, A.K. Chaudhuri, Phys. Status Solidi A 111 (1989) 515.

[23] L.L. Kazamerski, W.B. Berry and C.W. Allen, J. Appl. Phys., 43 (1972) 3515, 3521.

[24] J.C. Manifacier, J. Gasiot, J.P. Fillard, J. Phys. E: Sci. Instrum. 9 (1976) 1002.

[25] J.C. Manifacier, M. De Mucia, J.P. Fillard, E. Vicario, Thin Solid Films 14 (1977) 127.

[26] U. Pal, S. Saha, A.K. Chaudhuri, V.V. Rao, H.D. Banerjee, J. Phys. D: Appl. Phys. 22 (1989) 965.

[27] K. Ehsan, S.G. Tomlin, J. Phys. D: Appl. Phys. 8 (1975) 581.

[28] M.P. Lisitsa, L.F. Gudymenko, V.N. Malinko, S.F. Terekhova, Phys. Status Solidi 31 (1969) 389.

[29] J.L. Birman, Phys. Rev. 115 (1959) 1493.

[30] M. Cardona, M. Weinstein, G.A. Wolff, Phys. Rev. 140 (1965) A633.

[31] R. Lozada-Morales, O. Zelaya-Angel, Thin Solid Films 281 (1996) 386.

[32] G.D. Cody, T. Tiedje, B. Abeles, B. Brooks, Y. Goldstein, Phys. Rev. Lett. 47 (1981) 1480.

[33] L.V. Borkovskaya, B.R. Dzhumaev, N.E. Korsunskaya, I.V. Markevich, A.F. Singaevskii, Semiconductors 30 (1996) 400.

[34] M. Balkansi, I. Broser, Z. Elektrochem. 61 (1957) 715.

[35] G. Diemer, W. Hoogenstraaten, J. Phys. Chem. Solids 2 (1957) 119.